Analysis on Sound Field Recorded with Vector Sensors[1]

Fenghua Li, Mei Sun, and Renhe Zhang

State Key Laboratory of Acoustics, Institute of Acoustics, Chinese Academy of Sciences, Beijing 100190

Abstract. From data collected with vector sensors at several sites, the transmission losses of particle velocities and pressures are examined. In particular, the components of the particle velocity fields both normal and tangential to the horizontal plane are studied. Theoretical and experimental results show that both vertical and horizontal particle velocities can be regarded as the summation of normal modes. The lower modes dominate for the horizontal particle velocity, while higher modes are relatively important for the vertical particle velocity. The intensity of the vertical velocity decreases faster than that of the horizontal particle velocity. The experimental results also show that the same modes of the horizontal and vertical particle velocity have similar losses, but different amplitudes and phases. Theoretical analyses indicate that the difference of the mode amplitudes between horizontal particle velocity and vertical particle velocity depends on the eigenvalue and receiver depths, which can provide information on the estimation of bottom parameters. A geo-inversion scheme by the matched-field processing with a vector array is developed. The theoretical and experimental results indicate that the proposed inversion method can decrease the uncertainty of inversion in comparison with that by hydrophone arrays.

Keywords: Vector Sensor, Geo-acoustic Inversion, Normal mode
PACS: 43.30Bp, 43.30Re

INTRODUCTION

Vector sensors have attracted much attention in recent years. In comparison with hydrophone, vector sensors can provide measurements of three dimensional particle velocities, which have been widely used in the Direction of Arrival (DOA) estimation and improvement of Signal Noise Ratio (SNR)[1-4]. However, few papers have been published on the analyses of transmission losses of particle velocities and geo-acoustic inversion by vector sensors[5-6]. In this paper, based on normal mode theory, a concise expression of the transmission losses of vertical particle velocities have been derived. The theoretical results indicate that the vertical particle velocity has larger loss in comparison with the horizontal particle velocity, which is in agreement with the experimental results. A Matched Field Processing (MFP) with a vector sensor array has been applied to the data, which can reduce the inversion uncertainty in comparison with that of the hydrophone array.

[1] Supported by National Natural Science Foundation of China (10734100)

CP1272, *Shallow-Water Acoustics, Second International Shallow-Water Acoustics Conference*
edited by J. Simmen, E. S. Livingston, J. X. Zhou, and F. H. Li
© 2010 American Institute of Physics 978-0-7354-0822-7/10/$30.00

Downloaded 08 Oct 2010 to 159.226.100.225. Redistribution subject to AIP license or copyright; see http://proceedings.aip.org/about/rights_permissions

THEORY OF VECTOR FIELDS

With normal mode theory, the pressure, horizontal and vertical particle velocities excited by a homogenous point source can be expressed as

$$\mathrm{P} = \sqrt{\frac{8\pi}{r}} e^{i\pi/4} \sum_l \Phi_l(z_s)\Phi_l(z) \frac{1}{\sqrt{\mu_l}} e^{i\mu_l r - \beta_l r} \tag{1}$$

$$\mathrm{V}_r = i\sqrt{\frac{8\pi}{r}} e^{i\pi/4} \sum_l \Phi_l(z_s)\Phi_l(z)\sqrt{\mu_l} e^{i\mu_l r - \beta_l r} \tag{2}$$

$$\mathrm{V}_z = \sqrt{\frac{8\pi}{r}} e^{i\pi/4} \sum_l \Phi_l(z_s)\Phi_l{}'(z) \frac{1}{\sqrt{\mu_l}} e^{i\mu_l r - \beta_l r} \tag{3}$$

where r is the range between the source and receiver, $\Phi_l(z)$, μ_l and β_l are the eigenfunction, eigenvalue, and eigen-attenuation, ' denotes the derivation over z. $\mathrm{V_r}$ and $\mathrm{V_z}$ are the horizontal and vertical particle velocities, respectively. In this paper, the factor $i/(\rho\omega)$ has been neglected in the expression of $\mathrm{V_r}$ and $\mathrm{V_z}$.

By the smooth average theory, equations (1) to (3) in the Pekeris channel can be approximated as (in the three-half law region)

$$< |\mathrm{P}|^2 >= \left(\frac{\pi}{QH}\right)^{1/2} r^{-3/2} \tag{4}$$

$$< |\mathrm{V_r}|^2 >= k^2 \left(\frac{\pi}{QH}\right)^{1/2} r^{-3/2} \tag{5}$$

$$< |\mathrm{V_z}|^2 >= k^2 \left(\frac{\pi}{QH}\right)^{1/2} r^{-3/2} \frac{H}{2Qr} \tag{6}$$

It can be seen from Equations (4) to (6) that in general the vertical particle velocity $\mathrm{V_z}$ is much smaller than the horizontal particle velocity $\mathrm{V_r}$, and $\mathrm{V_z}$ has a larger loss than $\mathrm{V_z}$. Fig. 1 shows the comparison of the losses between the measured pressure, the horizontal and vertical particle velocities. The x-axis is the range between the source and the receiver, and the y-axis is the transmission loss. The circles are the measured pressures, and the triangles are the measured vertical particle velocities, the crosses are the measured horizontal particle velocities. The lines in the figure are the numerical simulations. It can be seen in the figure that the vertical particle velocity has a larger transmission loss than that of horizontal transmission loss, because high order normal modes contribute more to vertical particle velocity due to their large grazing angle; on the other hand, the low-order normal modes contribute more to the pressure and the horizontal particle velocity. It can also be seen in the figure that the measured data are in good agreement with the simulations.

Downloaded 08 Oct 2010 to 159.226.100.225. Redistribution subject to AIP license or copyright; see http://proceedings.aip.org/about/rights_permissions

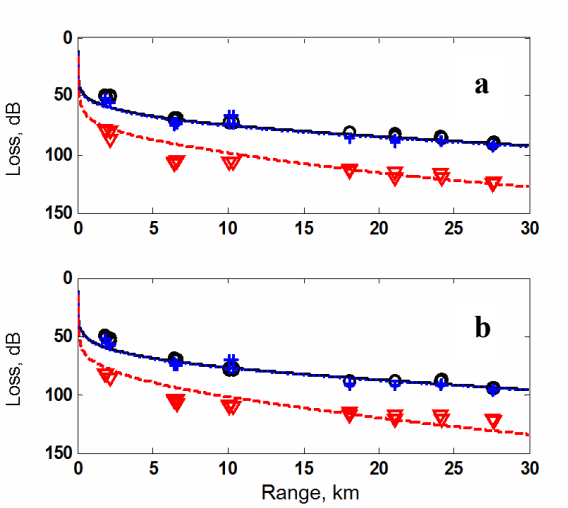

FIGURE 1. Measured and simulated pressure, particle velocities. (a): 600 Hz, (b): 800 Hz.

MODE ANALYSIS WITH VECTOR SENSOR

To further investigate the differences between the transmissions of the horizontal and vertical particle velocities, different mode amplitudes of the particle velocities are analyzed. Fig. 2 shows the sound speed profile measured in an experiment. An air-gun was used as a wide-band sound source from 5 km to 12 km. The depth of the vector sensor was 18.1 m, and the water depth was 32.5 m.

The recorded waveforms are shown in Fig. 3. The solid curves are the recorded waveforms and the dashed curves are the corresponding envelopes. The frequency range is from 100 Hz to 140 Hz. The range between the source and the receiver is 5.25 km. The upper plot is the measured horizontal particle velocity V_r, and the lower plot is the measured vertical particle velocity V_z. It can be seen clearly in the upper plot, which corresponds to V_r, that there are two normal modes in the recorded signal, and the amplitude of normal mode 1 is larger than that of normal mode 2. However in the lower plot, which corresponds to V_z, the amplitude of normal mode 1 is much smaller than that of normal mode 2. It can also be seen from the figure that the waveform of normal mode 2 of V_r has a $\pi/2$ phase shift with that of V_z.

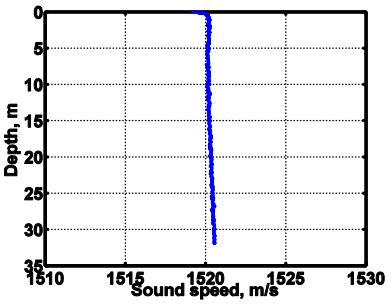

FIGURE 2. Measured sound speed profile.

Downloaded 08 Oct 2010 to 159.226.100.225. Redistribution subject to AIP license or copyright; see http://proceedings.aip.org/about/rights_permissions

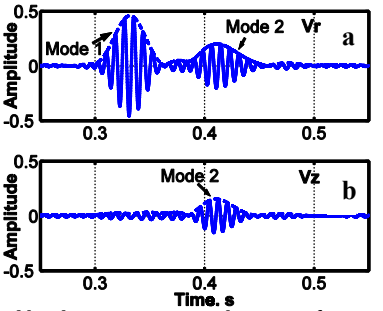

FIGURE 3. Waveform recorded by the vector sensor, the center frequency is 120 Hz. (a): Vr, (b): Vz.

The ratio between the amplitudes of the *l*th normal mode of V_r and V_z is defined as

$$RMHV_l = \frac{\text{Amplitude of } l\text{th mode of } V_r}{\text{Amplitude of } l\text{th mode of } V_z} = \frac{\Phi_l(z)\mu_l}{\Phi_l'(z)} \tag{7}$$

The measured ratios between the amplitudes of normal mode 2 of the horizontal and vertical particle velocity (RMHV) at 120 Hz (upper plot) and 200 Hz (lower plot) at different ranges are shown in Fig. 4. The circles are the measured RMHV. The lines are the average of all the measured RMHVs. It can be seen from Eq. 7 and Fig. 4 that the ratio $RMHV_l$ is a function of eigenfunction, eigenvalue, receiver depth, and independent of the range and source depth, which means that the same normal modes of the horizontal and vertical particle velocities have the same transmission losses. Fig. 3 also shows that high normal modes contribute more to the vertical particle velocity V_z than the horizontal particle velocity V_r. However, high normal modes have relatively larger transmission losses than the lower normal modes in general. Therefore, V_z has larger losses that V_r, which is in agreement with the measured data shown in Fig. 1.

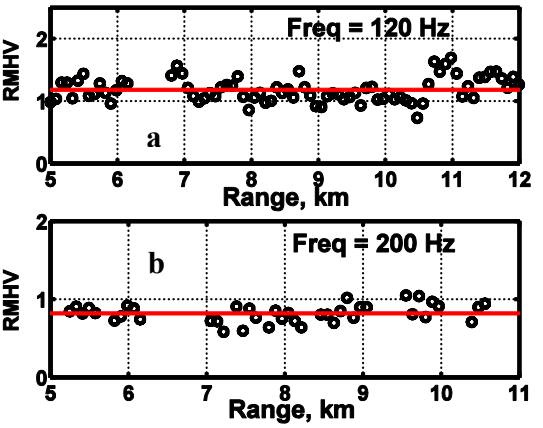

FIGURE 4. Measured RMHV at different ranges. (a): 120 Hz, (b): 200 Hz.

Downloaded 08 Oct 2010 to 159.226.100.225. Redistribution subject to AIP license or copyright; see http://proceedings.aip.org/about/rights_permissions

Since the vertical and horizontal particle velocities have different combinations of the normal modes, this information can be applied to geo-acoustic inversion. In this paper, matched-field processing with a vector sensor array is applied to estimate the bottom parameters. The cost function of MFP geo-acoustic inversion with hydrophones can be defined as

$$C_p = \frac{\sum_j \left| \sum_i P(z_i, f_j) Q^*(z_i, f_j) \right|}{\sqrt{\sum_j \sum_i P(z_i, f_j) P^*(z_i, f_j) \sum_j \sum_i Q(z_i, f_j) Q^*(z_i, f_j)}} \tag{8}$$

where $P(z_i, f_j)$ and $Q(z_i, f_j)$ are the measured and the simulated sound pressures at receiver depth z_i and frequency f_j.

Similarly, the cost function of MFP geo-acoustic inversion with pressure and vertical particle velocity is defined as

$$C_{p,v_z} = \sqrt{C_p \times \frac{\sum_j \left| \sum_i V_z(z_i, f_j) v_z^*(z_i, f_j) \right|}{\sqrt{\sum_j \sum_i V_z(z_i, f_j) V_z^*(z_i, f_j) \sum_j \sum_i v_z(z_i, f_j) v_z^*(z_i, f_j)}}} \tag{9}$$

where $V_z(z_i, f_j)$ and $v_z(z_i, f_j)$ are the measured and simulated vertical particle velocity at receiver depth z_i and frequency f_j.

To verify the differences between Eqs. (8) and (9), another shallow water acoustic experiment is performed. The experimental configuration is shown in Fig. 5. A four-vector-sensor array is used in the experiment. In the geo-acoustic inversion, a half-infinite liquid bottom model is used. The density and attenuation is set as 1.78 g/cm^3 by bottom core, and the attenuation is set as 0.02 dB/m since it is not sensitive to the MFP inversion. The frequency band used in the inversion is from 200 Hz to 300 Hz. Therefore the unknown parameters are the water depth and bottom sound speed. Fig. 6 shows the cost function as a function of the water depth and bottom sound speed. The ranges of the color bars in the figure are from the maximum of the calculated cost function minus 0.05 to the maximum. The cost function shown in the upper plot is defined by Eq. (8) and the cost function of the lower plot is defined by Eq. (9). It can be seen from the figure that the uncertainty of the MFP inversion with vector array is largely reduced in comparison with that of a hydrophone array.

Downloaded 08 Oct 2010 to 159.226.100.225. Redistribution subject to AIP license or copyright; see http://proceedings.aip.org/about/rights_permissions

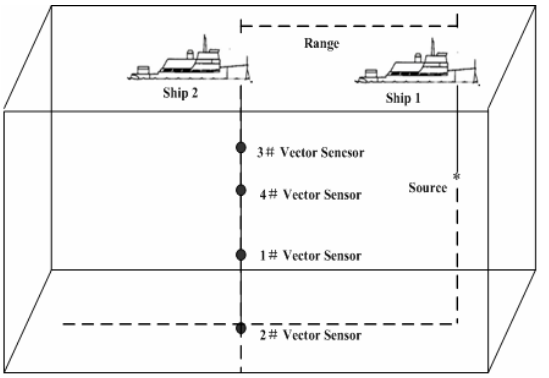

FIGURE 5. Experimental configuration.

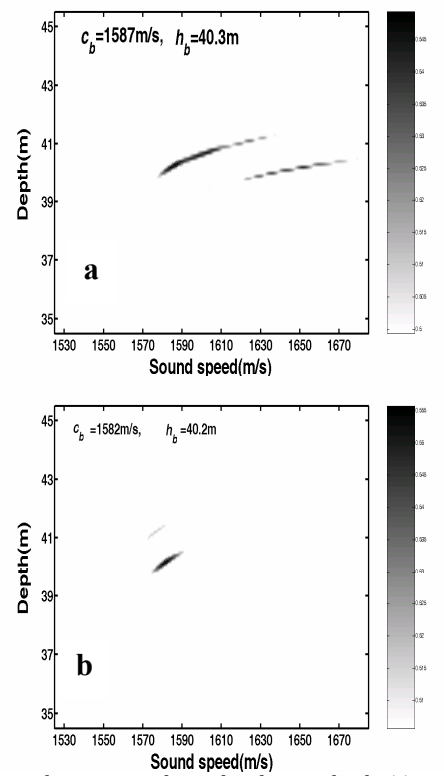

FIGURE 6. Cost function vs. bottom sound speed and water depth. (a): cost function defined as Eq.8, (b): cost function defined as Eq.9.

SUMMARY

The theoretical analyses and the experimental data show that the high order normal modes contribute more to vertical particle velocity due to their large grazing angle, and Vz has a larger loss than Vr. A MFP-based geo-acoustic inversion method has

Downloaded 08 Oct 2010 to 159.226.100.225. Redistribution subject to AIP license or copyright; see http://proceedings.aip.org/about/rights_permissions

been developed in this paper. The results indicate that the MFP method with a vector sensor array can reduce the uncertainty of inversion more effectively than a hydrophone array.

ACKNOWLEDGMENTS

This work is supported by the National Natural Science Foundation of China 10734100. The authors thank the staff who attended the sea experiment to obtain the valuable data for this paper.

REFERENCES

1. M. Hawkes and A. Nehorai, *IEEE trans on Signal Processing*, **46**, 2291-2304 (1998).
2. G. Sun and D. Yang, **Acta Acoustica**, **28**, 66-72 (2003) (in Chinese).
3. A. Nehorai, *IEEE trans on Signal Processing*, **42**, 2481-2491 (1994).
4. M. Hawkes and A. Nehorai, *IEEE Journal of Oceanic Engineering*, **26**, 337-347 (2001).
5. H. S. Peng and F. H. Li, *Chin. Phys. Lett.*, **24**, 1977-1980 (2007).
6. J. Y. Hui and H. Liu, *Acta Acoustica*, **25**, 303-307 (2000) (in Chinese).

Downloaded 08 Oct 2010 to 159.226.100.225. Redistribution subject to AIP license or copyright; see http://proceedings.aip.org/about/rights_permissions